Journal of Physiology (2002), **539.3**, *pp.* 657–668
DOI: 10.1013/jphysiol.2001.013432

www.jphysiol.org

Expression pattern and functional characteristics of two novel splice variants of the two-pore-domain potassium channel TREK-2

Wenli Gu *, Günter Schlichthörl †, Jochen R. Hirsch ‡, Hartmut Engels *, Christine Karschin §, Andreas Karschin §, Christian Derst †, Ortrud K. Steinlein * and Jürgen Daut †

* *Institut für Humangenetik, Universität Bonn, Wilhelmstrasse 31, D-53111 Bonn,* † *Institut für Physiologie, Universität Marburg, Deutschhausstrasse 2, D-35037 Marburg,* ‡ *Experimentelle Nephrologie, Universität Münster, Domagstrasse 2, D-48149 Münster and* § *Institut für Physiologie, Universität Würzburg, Röntgenring 9, D-97070 Würzburg, Germany*

Two novel alternatively spliced isoforms of the human two-pore-domain potassium channel TREK-2 were isolated from cDNA libraries of human kidney and fetal brain. The cDNAs of 2438 base pairs (bp) (TREK-2b) and 2559 bp (TREK-2c) encode proteins of 508 amino acids each. RT-PCR showed that TREK-2b is strongly expressed in kidney (primarily in the proximal tubule) and pancreas, whereas TREK-2c is abundantly expressed in brain. *In situ* hybridization revealed a very distinct expression pattern of TREK-2c in rat brain which partially overlapped with that of TREK-1. Expression of TREK-2b and TREK-2c in human embryonic kidney (HEK) 293 cells showed that their single-channel characteristics were similar. The slope conductance at negative potentials was 163 ± 5 pS for TREK-2b and 179 ± 17 pS for TREK-2c. The mean open and closed times of TREK-2b at −84 mV were 133 ± 16 and 109 ± 11 μs, respectively. Application of forskolin decreased the whole-cell current carried by TREK-2b and TREK-2c. The sensitivity to forskolin was abolished by mutating a protein kinase A phosphorylation site at position 364 of TREK-2c (construct S364A). Activation of protein kinase C (PKC) by application of phorbol-12-myristate-13-acetate (PMA) also reduced whole-cell current. However, removal of the putative TREK-2b-specific PKC phosphorylation site (construct T7A) did not affect inhibition by PMA. Our results suggest that alternative splicing of TREK-2 contributes to the diversity of two-pore-domain K^+ channels.

(Received 22 October 2001; accepted after revision 26 November 2001)
Corresponding author J. Daut: Institut für Physiologie, der Universität Marburg, Deutschhausstrasse 2, 35037 Marburg, Germany. Email: daut@mailer.uni-marburg.de

The family of two-pore-domain potassium (K_{2P}) channels is defined by their common structural features: the individual subunits have four transmembrane domains, two pore domains and a large M1–P1 linker (reviewed by Lesage & Lazdunski, 2000; Goldstein *et al.* 2001; Patel & Honore, 2001). Using homology analysis, five subfamilies of K_{2P} channels have been identified, the TWIK subfamily (Lesage *et al.* 1996*a*; Chavez *et al.* 1999; Salinas *et al.* 1999; Patel *et al.* 1999*b*), the THIK subfamily (Rajan *et al.* 2001), the acid-sensitive subfamily comprising TASK-1, -3 and -5 (Duprat *et al.* 1997; Kim *et al.* 1998, 2000; Rajan *et al.* 2000; Kim & Gnatenco, 2001; Karschin *et al.* 2001), the mainly alkaline-sensitive subfamily comprising TALK-1, TALK-2 and TASK-2 (Reyes *et al.* 1998; Decher *et al.* 2001; Girard *et al.* 2001), and the mechanosensitive subfamily comprising TREK-1, TREK-2 and TRAAK (Fink *et al.* 1996, 1998; Maingret *et al.* 1999*a,b*; Lesage *et al.* 2000*a,b*; Bang *et al.* 2000).

Most of the 14 mammalian K_{2P} channels identified so far are abundantly expressed in the brain (Talley *et al.* 2001). Since K_{2P} channels have been identified quite recently, less is known about their function compared with other K^+ channels. Nevertheless, four aspects that may be relevant for neuronal function have now become clear. (i) Some of the K_{2P} channels are modulated by changes in intracellular pH and may therefore play a protective role during cerebral ischaemia (Maingret *et al.* 1999*b*). (ii) Some of the K_{2P} channels are activated by volatile anaesthetics (Patel *et al.* 1999*a*; Gray *et al.* 2000; Lesage *et al.* 2000*b*; Sirois *et al.* 2000) and this may represent one of the major mechanisms responsible for the anaesthetic effect of halothane, chloroform, isoflurane and related drugs. (iii) Some of the K_{2P} channels can be activated by polyunsaturated fatty acids and by lysophospholipids (Fink *et al.* 1998; Lesage *et al.* 2000*a,b*; Maingret *et al.* 2000). It has been postulated that the release of polyunsaturated fatty acids following receptor-mediated stimulation of phospholipases may modulate synaptic transmission in the CNS (Fink *et al.* 1998). (iv) Some of the K_{2P} channels have been shown to be inhibited by activation of G-protein-coupled receptors, for example the M_3 muscarinic receptor (Millar *et al.*

2000), the thyrotrophin-releasing hormone receptor TRH-R1 (Talley *et al.* 2000) or the metabotrophic glutamate receptor mGluR1 (Lesage *et al.* 2000). Thus, K_{2P} channels could be the effectors of excitatory postsynaptic potentials elicited by activation of receptors coupled to G-proteins of the $\alpha_{q/11}$ subtype. Other transmitters that have been postulated to modulate the activity of K_{2P} channels include serotonin, noradrenaline (norepinephrine) and substance P (Talley *et al.* 2000).

The K_{2P} channel TREK-2 shares all of these functions (i–iv) and may therefore participate in many regulatory processes in the brain. Here we characterize two novel human splice variants of TREK-2, denoted TREK-2b and TREK-2c, which are differentially expressed in brain, kidney and pancreas. Since previous investigations of the related channel TREK-1 had shown that it can be modulated by protein kinase A (PKA) and protein kinase C (PKC) (Patel *et al.* 1998) we studied the possible function of the PKA and PKC phosphorylation sites of TREK-2b and TREK-2c using site-directed mutagenesis.

METHODS

Cloning of two splice variants of human TREK-2

A basic local alignment search tool (BLAST) search with the TREK-1 cDNA in the high throughput genomic sequences (HTGS) DNA database revealed a genomic fragment AL122021 (locus CNS01DSW) from human chromosome 14 that shares partial homology with TREK-1. The chromosomal localization of TREK-2 was confirmed by fluorescence *in situ* hybridization (data not shown). Reverse transcription-polymerase chain reaction (RT-PCR) was performed with human fetal brain total RNA (Clontech, Palo Alto, CA, USA) using the Titan One Tube RT-PCR system (Roche Molecular Biochemicals, Mannheim, Germany) and the primers:

5′-CCAAGTTGGTCTCCAATTCCAGCC-3′ (forward)

and 5′-GCGGGAGTCAGTCCAATAGGAAA-3′ (reverse).

The partial TREK-2 PCR product was cloned into the vector TOPO PCR2.1 (Invitrogen, Groningen, Germany) and sequenced. To obtain the entire TREK-2 cDNA, 5′ and 3′ rapid amplification of cDNA ends (RACE) was performed using Marathon-ready cDNA (Clontech) from human fetal brain and human kidney. Two 3′ nested primers:

5′-GCGGGAGTCAGTCAATAGGAAA-3′

and 5′-CAGCAGCCACTGGGACCTCGGCAG-3′

and two 5′ nested primers:

5′-CCTTCAGTGCTCGGAGCAATATTCCC-3′

and 5′-TCTTCTGGCTGCTCTCAAAGGGCTGCTCCAATGC-CCGGAAGA-3′

were used for amplification. The amplified products were cloned into the TOPO PCR2.1 vector and sequenced.

Cloning of rat TREK-1 and TREK-2c cDNAs

Two EST clones encoding partial human TREK-1 (AA464375, IMAGE-Id: 810165) and TREK-2 (AI073392, IMAGE-Id:1640332) cDNAs were labelled with digoxigenin and used for a non-radioactive screening of a λ-ZAP2 rat brain cDNA library using standard hybridization procedures and disodium 3-(4-methoxy-spiro(1,2-dioxetane-3,2′-(5′-chloro)tricyclo[3,3.1.1$^{3.7}$]decan)-4-yl) phenyl phosphate (CSPD) as a chemiluminescence substrate. After two further screenings for plaque purification, pBSK+ plasmids containing the TREK cDNAs were excised using the Exassist helper phage and completely sequenced.

Tissue distribution of the TREK-2 splice variants in different human tissues

The expression of three TREK-2 splice variants in different human tissues was analysed by PCR. The multiple-tissue cDNA panels Human I and Human II (Clontech) were used as templates. Sense primers corresponding to the first exons of the different splice variants were combined with the antisense primer located within the shared exon 2. Amplification products were designed to be of similar length to facilitate quantitative comparison. A second amplification was performed using two primers from the shared region to analyse the distribution of total TREK-2 expression. The primers used for each transcript were as follows. For TREK-2b:

FORb (5′-GCAAGGCATGGAGCCTGCACTTT-3′)

with BACK (5′-ACACCGGTGCTGCG GGAACGGCCA-3′);

for TREK-2c:

FORc (5′-TTCCTCCACGAGCCAGTCCAAGGCT-3′) with BACK;

and for TREK-2a:

FORa (5′-GGAGACTTTGCTCCACGATGTT-3′) with BACK.

Primers

5′-GCGGGAGTCAGTCCAATAGGAAAC-3′

and 5′-CCAAGTTGGTCTC CAATTCCAGCC-3′

from the part common to all three splice variants were used to analyse the total expression level of TREK-2. PCR was performed for 25 cycles of 2 s at 94 °C and 3 min at 68 °C with the polymerase Advantage 2 (Clontech).

The expression of TREK-2a in human total brain was additionally tested by nested RT-PCR from human fetal (Promega, Mannheim, Germany) and adult brain RNA (Clontech). The first RT-PCR step was carried out using the Titan One Tube RT-PCR system (Roche, Mannheim) according to the protocol of the manufacturer with an annealing temperature of 65 °C. The primers were

5′-GTTGCCAGAGATGACTGGGGTTTTCGGG-3′ and BACK.

Zero point zero two microlitres of the product was amplified again with the second pair of primers

5′-CGCAGGAACGCTAGGCAGTCTCT-3′

and 5′-GAAGTCTGTGTAGAGAAAAAACATCC-3′

using *Taq* polymerase (Invitrogen) and standard PCR conditions with an annealing temperature of 68 °C. All primers used in the distribution assays and RT-PCR were tested in combination with an antisense primer using genomic DNA. They all gave strong specific amplifications.

RT-PCR analysis of isolated of human nephron segments

Healthy cortical kidney pieces were obtained (with written consent) from patients undergoing tumour-nephrectomy. Nephron

segments were isolated using the procedure described previously for rat and rabbit kidney (Schafer *et al.* 1997). Selected tubules of a total length of 200 mm or glomeruli (400 pieces) were lysed in a 4 M guanidinium chloride buffer and total RNA was isolated using the RNeasy kit (Qiagen). Isolated total RNA was incubated with 10 units DNAse I (Promega, Heidelberg, Germany) at 37 °C for 1 h to digest traces of genomic DNA. RNA and DNase I were then separated by an additional cleaning step using a new RNeasy column. First strand cDNA synthesis was performed in a total reaction volume of 30 μl containing 5 μg total RNA, 10 mM dNTP-Mix, 1 nM $p(dT)_{10}$ nucleotide primer (Roche) and 200 units Moloney murine leukaemia virus (MMLV) reverse transcriptase (Promega). One-thirtieth of each cDNA first strand reaction mixture was then subjected to a 50 μl PCR reaction using 20 pmol of each primer (also used for the tissue distribution) and 1 unit of *Taq* DNA polymerase (Qiagen). Reaction conditions were as follows: 3 min at 94 °C, 30 s at 53 °C and 1 min at 72 °C, 1 cycle; 30 s at 94 °C, 30 s at 53 °C and 1 min at 72 °C, 30 cycles; 30 s at 94 °C, 30 s at 53 °C and 10 min at 72 °C, 1 cycle. All PCR products were directly sequenced to confirm correct amplification. For negative controls reverse transcriptase was omitted. Additionally, to exclude contamination, appropriate water controls excluding cDNAs were performed.

In situ hybridization of rat brain sections

Wistar rats were decapitated under ether anaesthesia, their brains were removed and frozen on powdered dry ice. Tissue was stored at −20 °C until cutting. Sixteen micrometre sections were cut on a Cryostat, thaw mounted onto silane-coated slides and air dried. After fixation for 10 min in 4 % paraformaldehyde dissolved in phosphate-buffered saline (PBS), slides were washed in PBS, dehydrated and stored in ethanol until hybridization.

Synthetic antisense oligonucleotides with least tendency of forming hairpins and self-dimers were chosen from the untranslated region and open reading frame (base positions on coding strand):

TREK-1,

(i) (125–172) 5′-CCCGCGAGGCGCTGGCAAGCATGAG-GCATGCAGCATTCAAAATGTTTG-3′,

(ii) (197–244) 5′-TGGAGTTCTGAGCAGCAGACTTGGGA-TCCAGCAAGTCAGGGGCCGCCA-3′,

(iii) (1262–1308) 5′-CACCGACAGGGTCCTCCTACATGGAG-TCAGTTCCTGGTTATGGTTAC-3′;

TREK-2c,

(i) (199–245) 5′-CTTGAAGTGGCTCGTGGGGAGCCCG-GGAGAAAGATAAGCGGGAAAAT-3′,

(ii) (344–391) 5′-CTTGGCGTCTCGATTGGAAATTTCAT-TGCTCCGTTGCCCACAGGGGGG-3′,

(iii) (1904–1952) 5′-CTCCAGCCCCTGGTCTTTGGTGTCCA-TGGGTACCATTCCATTCTCCATC-3′.

Three specific oligonucleotides corresponding to different 3′ and 5′ regions of the cDNAs were generated to exclude cross-hybridization between different K_{2P} subunits and to detect possible discrepancies related to the existence of additional N- or C-terminal splice variants.

Oligonucleotides were 3′ end-labelled with [^{33}P]dATP (New England Nuclear, Boston, MA, USA; 1000 Ci mmol^{-1}) by terminal deoxynucleotidyl transferase (Roche Diagnostics) and used for hybridization at concentrations of 2–10 pg μl^{-1} (4×10^5 c.p.m. (100 μl)$^{-1}$ hybridization buffer per slide). Control sections were (a) hybridized with sense oligonucleotide probes, (b) digested with RNase A (50 ng ml^{-1}) for 30 min at 37 °C before hybridization, and (c) hybridized with a mixed oligonucleotide probe containing a 20- to 50-fold excess of unlabelled probe. Slides were air dried and hybridized for 20–24 h at 43 °C in 100 μl buffer containing 50 % formamide, 10 % Dextran sulfate, 50 mM DTT, 0.3 M NaCl, 30 mM Tris–HCl, 4 mM EDTA, 1 × Denhardt's solution, 0.5 mg ml^{-1} denatured salmon sperm DNA, and 0.5 mg ml^{-1} polyadenylic acid and labelled oligonucleotide probe. Sections were washed 2 × 30 min in 1 × SSC plus 50 mM 2-mercaptoethanol, 1 h in 1 × SSC at 60 °C, and 10 min in 0.1 × SSC at room temperature. Specimens were then dehydrated, air dried and exposed to Kodak BIOMAX x-ray film for 16–21 days. For cellular resolution, selected slides were dipped in photographic emulsion, incubated for 6–10 weeks and then developed in Kodak D-19 for 3 min.

Expression of TREK channels in HEK 293 cells

The entire hTREK-2b and hTREK-2c coding regions were cloned into the expression vector pcDNA3.1 and transfected into HEK 293 cells using lipofectamine 2000 (Life Technologies). Electrophysiological recordings were made using with an Axopatch 200B amplifier (Axon Instruments). The sampling rate was usually 16 kHz and the cut-off frequency of the low-pass filter was 10 kHz (−3 dB). In some experiments the sampling rate was increased to 100 kHz. Pipettes with resistances of 5–8 MΩ were used for cell-attached and whole-cell measurements. The pipettes were coated with R6101 elastomer from Dow Chemicals. Single-channel measurements were performed with a pipette solution containing (mM): 140 KCl, 1 EGTA and 10 Hepes (divalent cation-free solution) or 145 KCl, 1 $MgCl_2$, 1 $CaCl_2$ and 5 Hepes (divalent cation-containing solution). The bath solution for the single-channel measurements contained (mM): 60 KCl, 85 NaCl, 1 $MgCl_2$, 0.33 NaH_2PO_4, 5 Hepes and 10 glucose. In this solution, the average membrane potential was approximately −4 mV. Whole-cell measurements were carried out with a pipette solution containing (mM): 65 potassium glutamate, 50 KCl, 10 KH_2PO_4, 7.9 $MgCl_2$, 5 EDTA, 5 Hepes, 1.9 K_2ATP and 0.2 Na_3GTP. The bath solution for the whole-cell measurements contained (mM): 5 KCl, 140 NaCl, 10 Hepes, 10 glucose, 1 $MgCl_2$, 1 $CaCl_2$, 0.33 NaH_2PO_4 and 2 sodium pyruvate. The membrane potential measurements were not corrected for the liquid junction potential, determined as described by Neher (1992), which was +2.8 mV.

RESULTS

Cloning of two novel human TREK-2 splice variants

Using a RACE strategy we isolated two novel human TREK-2 splice forms, denoted TREK-2b and TREK-2c, from human kidney and brain, respectively. The isolated cDNAs of 2438 base pairs (bp) (TREK-2b, GenBank accession number AF385399) and 2559 bp (TREK-2c, GenBank accession number AF385400) both code for proteins of 508 amino acids. At the amino acid level the proteins are 66 % identical to human TREK-1 and 47 % identical to human TRAAK. TREK-2b and TREK-2c differ significantly in their 5′-UTR and in the coding region for the first 17 amino acids. These regions also differ significantly from a previously isolated human TREK-2

splice variant (Lesage *et al.* 2000*b*; GenBank accession number: AF279890), here referred to as TREK-2a (Fig. 1*B*). The differences are due to alternative usage of the first exon. The alternative exons were localized by BLAST search in a human genomic database entry; the predicted gene structure is indicated in Fig. 1*A*. Interestingly, TREK-2b harbours a PKC phosphorylation site in the N-terminal part that is not present in the other two splice variants.

Cloning of rat brain TREK isoforms

cDNAs encoding the rat orthologues of TREK-1 and TREK-2c (rTREK-1 and rTREK-2c) were isolated from a rat brain cDNA library. The cDNAs of 3291 bp (rTREK-1, GenBank accession number AF385401) and 3056 bp (rTREK-2c, GenBank accession number AF385402) code for predicted proteins of 426 amino acids (rTREK-1) and 538 amino acids (rTREK-2), respectively, which were 60.7 % identical to each other at the amino acid level. Whereas the coding region of the rTREK-2c cDNA was identical to a recently described isoform (Bang *et al.* 2000), the rTREK-1 cDNA showed a 15 amino acid extension compared with the human TREK-1 sequences described previously (Fink *et al.* 1996; Meadows *et al.* 2000). However, another human GenBank entry (AF004711) encoding a TREK-1 isoform (named TPKC-1) from human brain shows a similar extension at the N-terminus and a different 5′ UTR compared with the shorter TREK-1 splice form (Bockenhauer *et al.* 2001). This may indicate alternative splicing of the human TREK-1 gene in which the start codon of the shorter splice form is split by an intron. A similar alternative N-terminal splicing may also take place in the TRAAK gene (compare Lesage *et al.* 2000*a* and GenBank entry AF247042).

Tissue distribution of human TREK-2 splice forms

The expression of TREK-2 splice variants in different human tissues was analysed by PCR of multiple-tissue cDNA panels Human I and II from Clontech. As shown in Fig. 2, TREK-2b is strongly expressed in kidney and pancreas. Only very faint signals could be observed in lung, liver and skeletal muscle. TREK-2c is strongly expressed in adult brain, while weak expression could also be observed in other tissues. In panel Human II, none of the three primers gave any PCR product (not shown). Using the same experimental procedure, no transcripts of TREK-2a could be identified in either cDNA panel, suggesting that it is not or very weakly expressed in these tissues (data not shown). Since TREK-2a was originally cloned from human brain RNA (Lesage *et al.* 2000*b*) we performed nested RT-PCR of both human fetal and adult brain RNA. TREK-2a primers amplified a splice variant-specific fragment of 139 bp which was subsequently confirmed by sequencing. Thus, TREK-2a is expressed in brain, but at a much lower level than TREK-2c.

Amplification with two primers from the shared part of the variants was used to estimate the total amount of TREK-2 expression. The strongest signal was observed in kidney, followed by brain and pancreas (Fig. 2). In all other

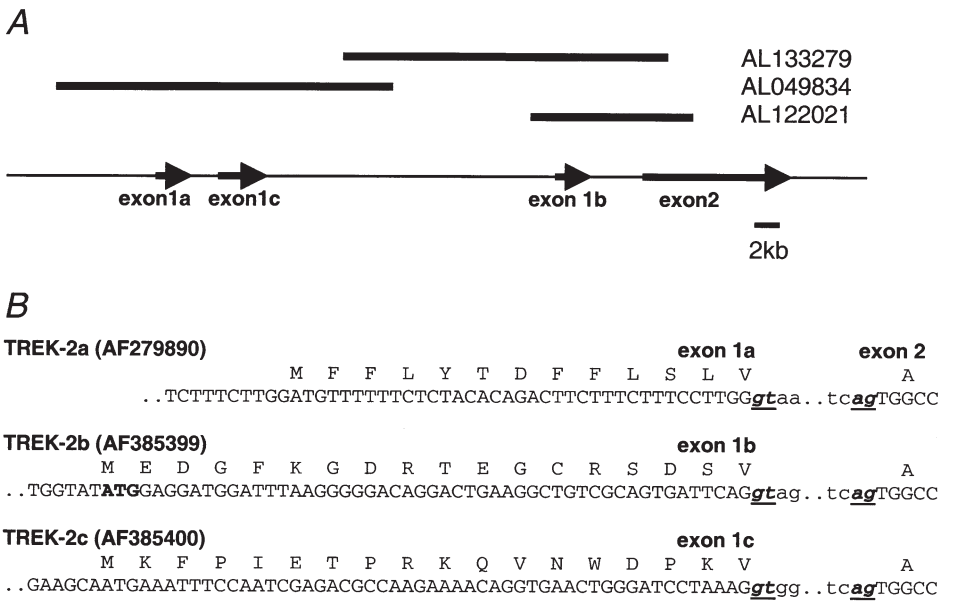

Figure 1. Sequence analysis of TREK-2 splice forms

A, relative orientation of the first exons of the splice variant identified in kidney (TREK-2b), fetal brain (TREK-2c) and the variant reported by Lesage *et al.* 2000*b* (TREK-2a). The corresponding genomic contigs are also shown. Exons are not drawn to scale. *B*, N-terminal cDNA and amino acid sequences of the human TREK-2 splice variants (accession numbers are given in brackets). The start codon (bold) and the splice sites of the first intron (underlined) are indicated. cDNA sequences are shown in capital letters, intronic sequences in lower case letters.

Table 1. Distribution of TREK-1 and TREK-2c mRNA in the adult rat brain

Brain region	TREK-2c	TREK-1	Brain region	TREK-2c	TREK-1
Olfactory bulb granule cell layer	+++	+	Thalamus: anteromedial nuclei	+++	+++
Olfactory tubercle	0	+++	Central grey	+	+++
Piriform cortex	+++	+++	Dorsal raphe nucleus	++	+++
Tenia tecta, Indusium griseum	0	++++	Interpeduncular nucleus	+	+++
N. of the lateral olfactory tract	++	+++	Cerebellum: deep nuclei	0	0
Neocortex	+	++	Cerebellum: Purkinje cells	0	0
Neocortex layer IV	+	+++	Cerebellum: granule cell layer	++++	+
Hippocampus dentate gyrus	+++	++	Pontine nucleus	+++	0
CA1 pyramidal cells	++	++	Medioventral periolivary n.	0	+++
CA2 pyramidal cells	++	++++	Trapezoid body	+++	0
CA3 pyramidal cells	++	0	Superior olivary nuclei	+	0
Caudate putamen	0	+++	Locus coeruleus	++++	0
Nucleus accumbens	0	+++	Dorsal tegmental nuclei	++	+++
Globus pallidus	0	0	Gigantocellular reticular n.	++++	0
Medial amygdaloid nuclei	+	++++	Spinal trigeminal nucleus	+++	±
Hypothalamus	+	++	Motor trigeminal nucleus	++	+++
Arcuate nucleus	+	+++	Facial nucleus	few+++	few+++
Preoptic nuclei	+	+++	Hypoglossus nucleus	++	++
Supraoptic nucleus	+++	+	Dorsal motor n. of the vagus	+++	+++
Habenula, medial nuclei	++	±	Solitary nucleus	++	+++
Thalamus: reticular nucleus	+	+++	Area postrema	+	++++
Thalamus: paraventricular nuclei	+++	+++	Inferior olive	0	++

In situ hybridization signals obtained for ^{33}P-labelled oligonucleotide probes on adult rat brain sections were rated according to the relative grain density: ++++, very abundant; +++, abundant; ++, moderate; +, low; ±, just above background; 0, no expression; few, only a few cells are labelled. Note that only selected brain regions with elevated expression levels or markedly differential expression patterns are included in the table.

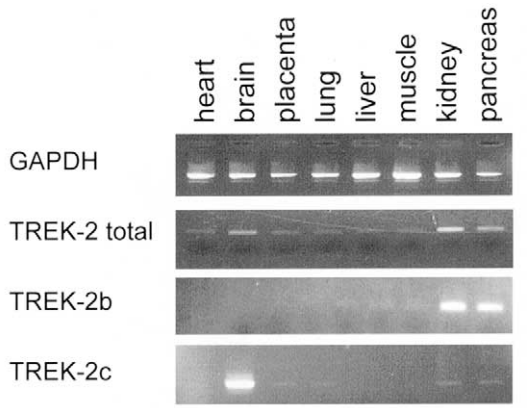

Figure 2. Tissue distribution of human TREK-2b and TREK-2c

Multiple-tissue cDNA panels from Clontech were used to study the tissue distribution of the three TREK-2 isoforms. To avoid possible genomic contamination, we used splice variant-specific primer pairs that included an exon–intron boundary fragment. In panel Human I, 180 bp fragments were amplified by specific TREK-2b and TREK-2c primers, whereas no PCR product could be observed with specific TREK-2a primers (not shown). Note that the TREK-2b signals in lung, liver and muscle were very faint. All cDNAs were also tested for GAPDH expression, and negative controls were performed with all RNA samples to exclude contamination.

tissues, weak but distinct expression could be seen. This result is in good agreement with the previously reported distribution pattern of TREK-2 expression. The strong expression of TREK-2 in kidney suggests that this K^+ channel may play a role in transepithelial transport. Therefore we analysed the expression of TREK-2b in different segments of human nephrons. In isolated human tubular fragments TREK-2b was strongly expressed only

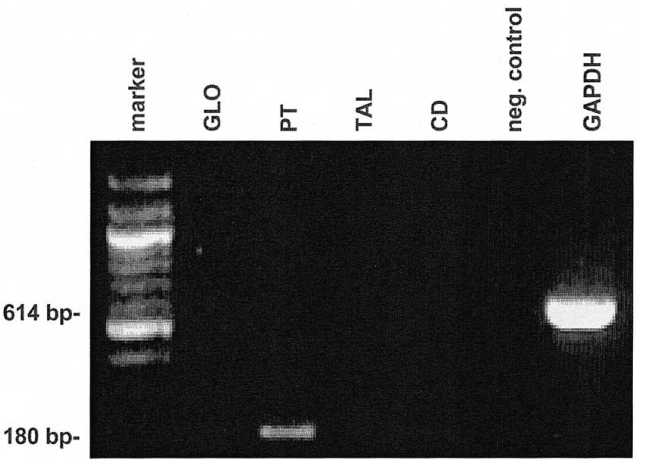

Figure 3. Expression of TREK-2b in human kidney

RT-PCR analysis of human glomeruli (GLO), proximal tubule (PT), thick ascending limb (TAL) and cortical collecting duct (CD). Molecular weight markers are shown in the left lane.

in the proximal tubule, as illustrated in Fig. 3. A faint expression was also detected in the collecting duct (not shown). No expression was found in the thick ascending limb and in glomeruli.

TREK-1 and TREK-2c localization in rat brain

Using *in situ* hybridization we compared the mRNA expression pattern of the brain-specific TREK-2c splice variant with the expression pattern of TREK-1 in the adult rat brain (Table 1, Fig. 4). In these experiments probe specificity was ensured by identical hybridization patterns of three oligonucleotides for each TREK-1 and TREK-2 in rat brain, as well as complete overlap with signals obtained from mouse-specific oligonucleotide probes in mouse brain.

As summarized in Table 1, TREK-2c hybridization signals were present throughout the brain. Of special note, high TREK-2c mRNA expression levels coincide with strong expression of TREK-1 mRNA in various nuclei, such as the nucleus of the lateral olfactory tract and the piriform cortex in the forebrain, the paraventricular and anteromedial thalamic nuclei, and in the brainstem the dorsal tegmental nuclei, solitary nucleus, and dorsal nucleus of the vagus. On the other hand, strong TREK-2c signals are also found in brain regions where TREK-1 mRNA is virtually absent. These include the granule cell layers of the cerebellum and olfactory bulb, as well as particular brainstem nuclei, e.g. pontine nucleus, trapezoid body, locus coeruleus, spinal trigeminal nucleus and gigantocellular neurons throughout the reticular formation. Note that vice versa many regions such as caudate putamen, nucleus accumbens, neocortex layer IV or interpeduncular nucleus specifically express only TREK-1 mRNA. Both TREK-1 and TREK-2b were found to be absent from fibre pathways, in which only glial labelling is expected.

Electrophysiological characterization of TREK-2 splice forms

For analysis of channel function TREK-2b and TREK-2c were heterologously expressed in HEK 293 cells. Single-

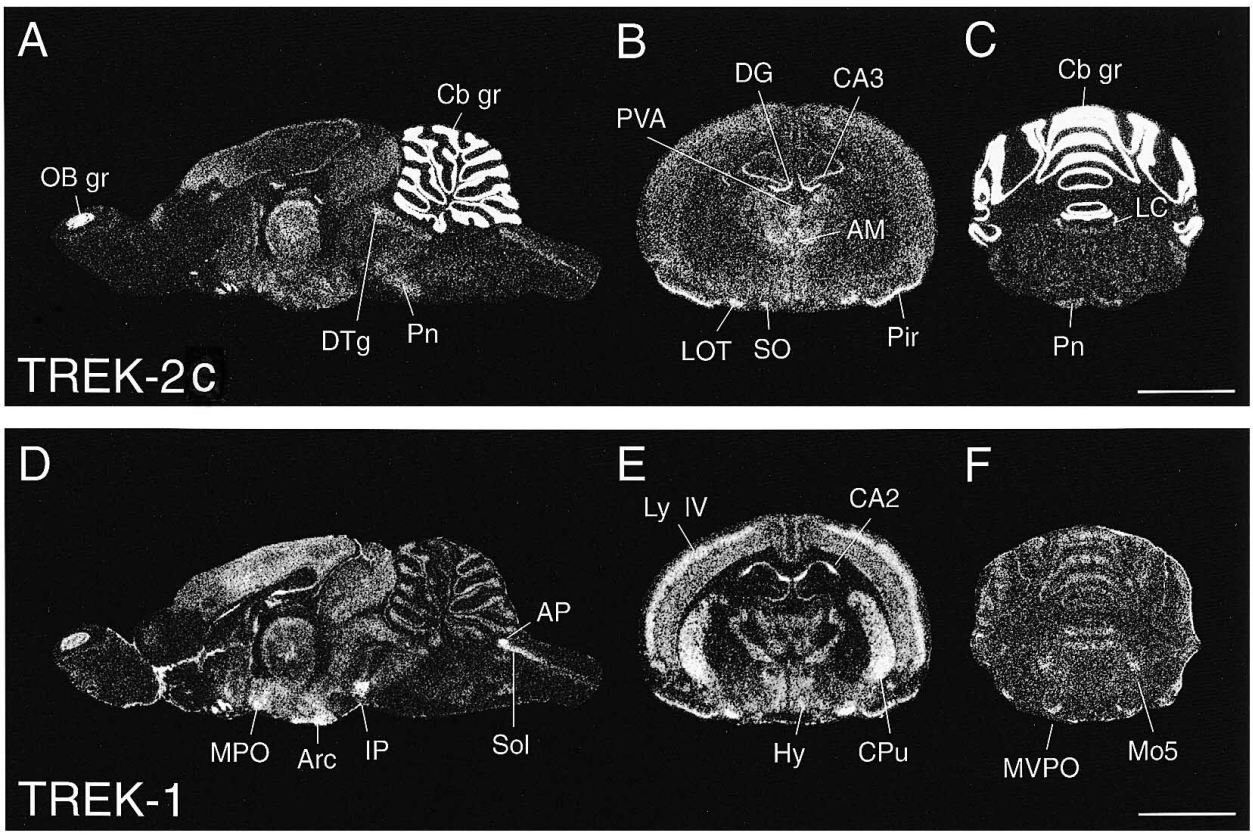

Figure 4. Distribution of TREK-2c and TREK-1 transcripts in rat brain

A–C, TREK-2c; *D–F*, TREK-1. X-ray film images show the differential expression patterns in adjacent midsagittal sections (*A* and *D*), and in coronal forebrain (*B* and *E*) and brainstem (*C* and *F*) sections. AM, anteromedial thalamic n.; AP, area postrema; Arc, arcuate n.; CA2 and CA3, hippocampal pyramidal cells of the corresponding region; Cb gr, cerebellar granule cell layer; CPu, caudate putamen; DG, hippocampus dentate gyrus; DTg, dorsal tegmental n.; Hy, hypothalamus; IP, interpeduncular n.; LC, locus coeruleus; LOT, n. of the lateral olfactory tract; Ly IV, neocortical layer IV; Mo5, motor trigeminal n.; MPO, medial preoptic n.; MVPO, medioventral periolivary n.; OB gr, olfactory bulb granule cell layer; Pir, piriform cortex; Pn, pontine n.; PVA, paraventricular thalamic n.; SO, supraoptic n.; Sol, solitary n., where n. stands for nucleus; scale bars represent 5 mm.

channel recordings showed channels with the characteristic high-frequency flicker of two-pore-domain K^+ channels (Fig. 5*A*). The all-points histogram (Fig. 5*B*) illustrates that not all of the rapid closures could be resolved at a sampling rate of 16 kHz. The amplitude of the single-channel currents was determined using an algorithm which excludes the short events, as illustrated in Fig. 5*C*. This method allows precise determination of single-channel conductance even in channels with rapid kinetics. The longer closed times could not be determined because most patches contained more than one channel. The open and closed times responsible for the flicker could be analysed during episodes in which only one channel was open (Fig. 5*A*). Typical open and closed time distributions are shown in Fig. 5*D* and *E*. At −84 mV, the mean open time of TREK-2b was 133 ± 16 μs ($n = 4$), the short mean closed time of TREK-2b was 109 ± 11 μs ($n = 4$). Similar data were obtained for TREK-2a and in recordings in which the sampling rate was increased to 100 kHz ($n = 4$, not illustrated).

In symmetrical potassium solution the dependence of the single-channel current on potential was found to be

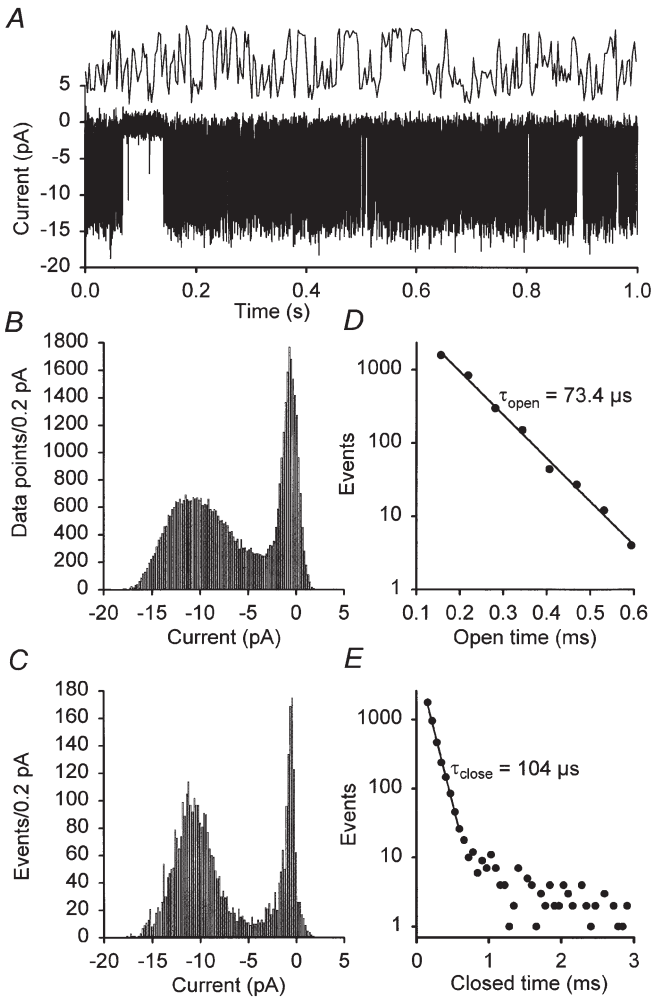

Figure 5. Single-channel recordings of TREK-2c

A, typical cell-attached recording of a TREK-2c channel expressed in HEK 293 cells. The top trace shows the first 20 ms of the lower trace at 50 × higher time resolution. *B*, all-points amplitude histogram of a typical cell attached record form a patch containing only one TREK-2c channel. *C*, event amplitude histogram constructed from the same set of data using an algorithm that excludes very short events, i.e. only events with a duration of more than 0.3 ms (> 5 data points) were included. *D*, typical open time distribution. *E*, closed time distribution of the same recording. In *A*–*E* the transmembrane potential (inside–outside) was −84 mV, the sampling rate was 16 kHz, and the pipette solution contained no divalent cations.

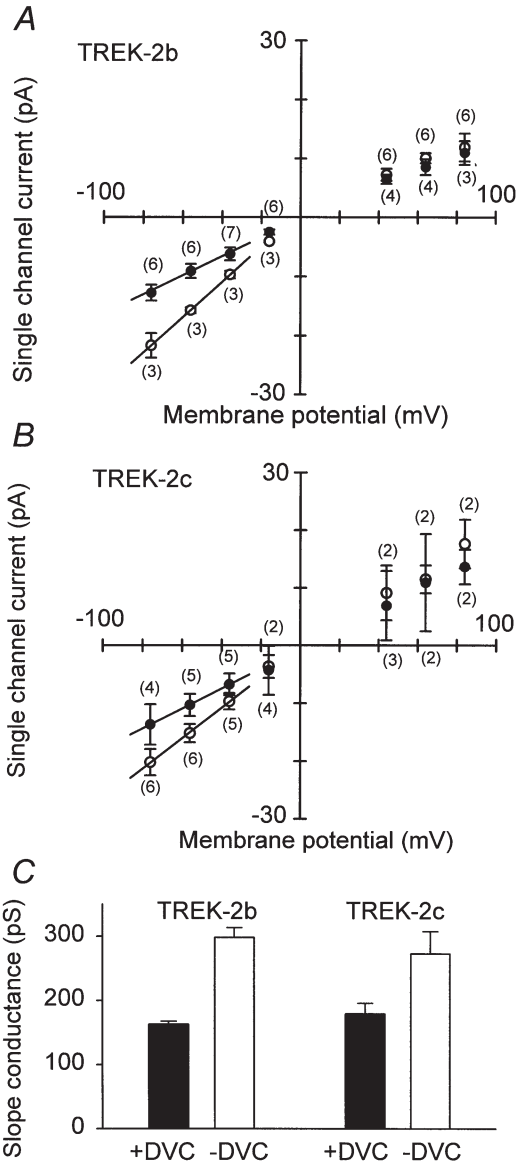

Figure 6. Dependence of single-channel conductance on external Ca^{2+}

A, single-channel current–voltage relation of TREK-2b and TREK-2c in the presence (●) and in the absence (○) of external divalent cations. *B*, mean values of the slope conductance of TREK-2b and TREK-2c, determined between −80 and −40 mV in the presence (●) and in the absence (○) of external divalent cations. *C*, the slope conductance of TREK-2b and TREK-2c measured in the presence (+DVC) and in the absence (−DVC) of external divalent cations.

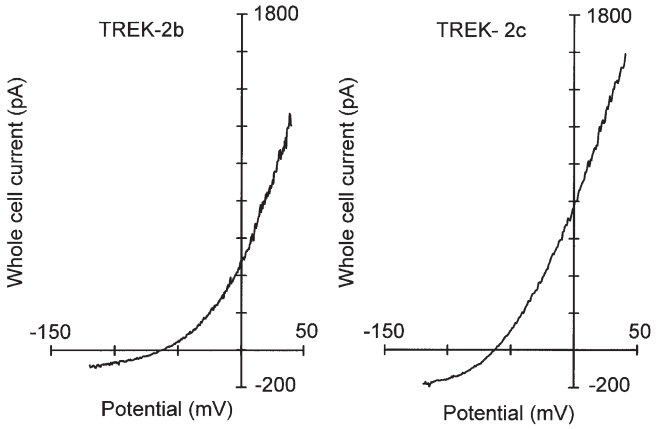

Figure 7. Whole-cell currents through TREK-2b and TREK-2c channels

Typical whole-cell currents in physiological salt solution (containing 5 mM K^+) observed after transfection of HEK 293 cells with TREK-2b or TREK-2c.

almost linear in the presence of divalent cations in the pipette solution (Fig. 6*A* and *B*). The slope conductance between −76 and −36 mV was found to be 163 ± 5 pS for TREK-2b and 179 ± 17 pS for TREK-2c. For both splice forms the slope conductance was significantly larger in the absence of external divalent cations, for TREK-2b it was 298 ± 16 pS and for TREK-2b it was 273 ± 35 pS. In all cases, the difference between the two splice forms was not statistically significant ($P > 0.05$; Fig. 6*C*). Our results clearly show that in divalent cation-free solution both TREK-2b and TREK-2c showed inward rectification at the single-channel level.

Whole-cell recordings of HEK 293 cells transfected with TREK-2 channels show strong outward rectification in physiological salt solution containing 5 mM K^+ and divalent cations, as illustrated in Fig. 7. Since TREK-2a has been shown to be activated by volatile anaesthetics (Lesage *et al.* 2000*a*) we tested the effects of isoflurane, chloroform and halothane on the whole-cell currents produced by the novel splice variants TREK-2b and TREK-2c (not illustrated). In the voltage range tested (−120 to +40 mV) the currents of the transfected cells were reversibly increased by isoflurane and halothane, in agreement with the results reported for TREK-2a. At 0 mV, the outward current produced by TREK-2b or TREK-2c was increased by 34.5 ± 5.5 % ($n = 5$) in the presence of 1 mM halothane and by 12.0 ± 6.7 % in the presence of 1 mM isoflurane ($n = 3$). No difference between TREK-2b and TREK-2c in the sensitivity to volatile anaesthetics was found. We also tested whether the novel splice forms of TREK-2 could be stimulated by externally applied lipids. In agreement with previous work on TREK-2a (Lesage *et al.* 2000*b*) we found that the whole-cell currents produced by TREK-2b and TREK-2c could be increased by application of 10 μM linoleic acid (60 ± 26 %; $n = 3$) or 10 μM arachidonic acid (62 ± 13 %; $n = 3$). These data suggest that the pharmacological properties of the TREK-2 channels are unaltered by the alternatively spliced N-terminus.

TREK-2c has a putative PKC phosphorylation site (at position 7) not present in TREK-2b and TREK-2a. Therefore we tested the effects of PKC phosphorylation (induced by application of phorbol-12-myristate-13-acetate, PMA) on TREK-2b and TREK-2c whole-cell currents (Fig. 8). The currents were inhibited by PMA in the voltage range tested, as illustrated in Fig. 8*B*. At 0 mV, 40 nM PMA decreased TREK-2b outward currents to 51 ± 5 % of control and TREK-2c currents to 57 ± 10 % of control. Exchange of the putative TREK-2c PKC phosphorylation site (TREK-2c T7A) did not change inhibition by PMA (Fig. 8*B*, *inset*), indicating that this effect is mediated by

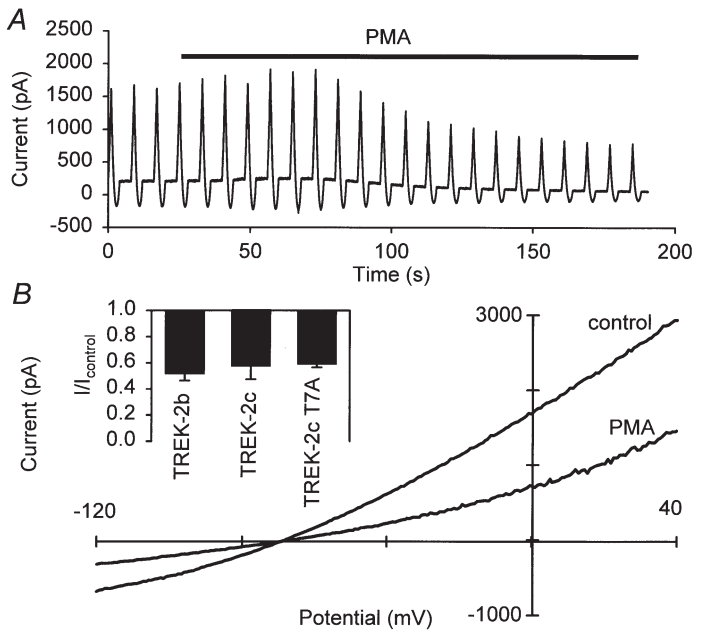

Figure 8. Effects of protein kinase C activation

A, typical recording of the effects of 40 nM PMA on the whole-cell current carried by TREK-2c; repetitive voltage ramps between −120 and +40 mV were applied. *B*, comparison of the current–voltage relation obtained under control conditions and in the steady state after application of PMA. *Inset*, comparison of the effects of 40 nM PMA on the currents produced by TREK-2b, TREK-2c and TREK-2c T7A.

one or more PKC phosphorylation sites shared by both splice forms.

It has been shown previously that the TREK-1 current amplitude is also down-modulated by PKA phosphorylation at the serine residue at position 333 (Patel *et al.* 1998; Lesage *et al.* 2000*b*). Since this PKA site is conserved in TREK-2 (serine 364) we tested the effects of PKA phosphorylation induced by forskolin (Fig. 9). Application of 10 μM forskolin produced a significant decrease in whole-cell current in both TREK-2b (to 57 ± 7 % of control) and TREK-2c (to 64 ± 13 % of control). When the single PKA phosphorylation site was removed (TREK-2c S364A) treatment of the cells with forskolin had no effect (95 ± 7 % of control) as illustrated in Fig. 9*B inset*. These data suggests a direct effect of the phosphorylation of residue 364 on TREK-2b and TREK-2c channels.

DISCUSSION

Tissue distribution of TREK-2 channels

The two novel splice forms of TREK-2 reported here showed a clearly distinct expression pattern: whereas TREK-2b is strongly expressed in kidney and pancreas, TREK-2c is mainly expressed in brain. This may indicate differentially regulated alternative splicing of the TREK-2 pre-mRNA in different tissues. We were not able to detect the originally described splice form, TREK-2a (Lesage *et al.* 2000*b*), in any of the multiple-tissue cDNA panels tested. However, RT-PCR of human RNA indicated a very low level of expression of TREK-2a in fetal and adult brain, which was only detectable after re-amplification of the original RT-PCR products.

We have found a differential expression pattern for TREK-1 and TREK-2c mRNAs in rat brain (Fig. 4 and Table 1). In some areas of the brain the transcripts of TREK-1 and TREK-2c were found to have an overlapping distribution, whereas in other areas only transcripts of one of the channels could be detected. The expression pattern of TREK-2c described here may be compared with the *in situ* hybridization data obtained very recently by Talley *et al.* (2001) with non-specific TREK-2 oligonucleotides that did not discriminate between different splice variants. Despite quantitative differences, the results of Talley *et al.* (2001), which probably also represent the regional distribution of the splice variant TREK-2c, are in reasonable agreement with our data in many brain regions. However, there are also some remarkable discrepancies. In our analysis, for example, various brainstem nuclei, e.g. the dorsal motor nucleus of the vagus, solitary nucleus and hypoglossus nucleus were found to contain high levels of TREK-2c transcripts. Furthermore, we detected strong expression levels of TREK-2c in the paraventricular and anteromedial thalamic nuclei as well as in the pontine nucleus. Another striking difference is that in our study strong TREK-2c signals were observed in the locus coeruleus, whereas Talley *et al.* report signals very close to background in this area. The locus coeroleus contains most of the noradrenergic neurons of the CNS with a broad efferent network, thus providing a well-characterized neural system suitable for the functional characterization of TREK-2c.

It is generally agreed that quantitative comparison of expression levels of different channels is difficult because the hybridization efficiencies of oligonucleotide and RNA probes may depend not only on the design of the probe and methodological details but also on local cellular factors. In view of these experimental limitations it is gratifying to see that by and large the results obtained by Talley *et al.* (2001) and by our group are consistent.

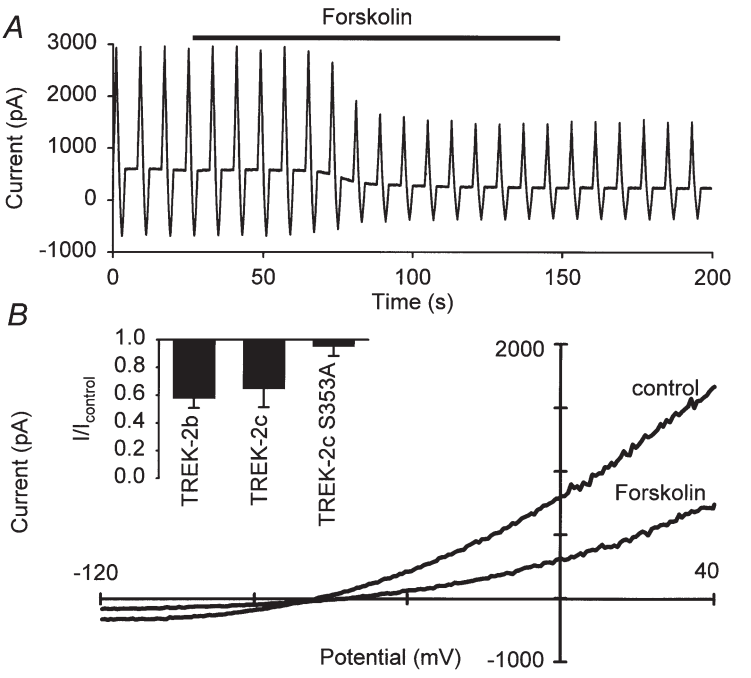

Figure 9. Effects of protein kinase A activation

A, typical recording of the effects of 10 μM forskolin on the whole-cell current carried by TREK-2c; repetitive voltage ramps between −120 and +40 mV were applied. *B*, comparison of the current–voltage relation obtained under control conditions and in the steady state after application of forskolin. *Inset*, comparison of the effects of 10 μM forskolin on the currents produced by TREK-2b, TREK-2c and TREK-2c S353A.

Together, these studies may contribute to the endeavour of correlating heterogeneity of channel expression with heterogeneity of physiological properties of different populations of neurons.

The other splice variant, TREK-2b, was strongly expressed in the proximal tubule of human kidney. To elucidate the possible function of these channels in the kidney it is necessary to determine the subcellular localization of TREK-2b channels. If they are targeted to the basolateral membrane their strong outward rectification would be consistent with a role of these channels in the transepithelial transport of potassium ions.

Functional characteristics of TREK-2 channels

Using an algorithm that excluded the very short events we were able precisely to determine the current amplitudes of TREK-2b and TREK-2c channels at different potentials despite the rapid kinetics of the channels. In symmetrical K^+ solution, the single-channel current voltage relation of both splice forms was almost linear in the presence of external Ca^{2+} and Mg^{2+}. The slope conductance measured at negative potentials in the presence of divalent cations was in the range 150–200 pS. Since the longer events showed a roughly Gaussian distribution and were consistent with the histogram of the raw data (Fig. 5) it is very unlikely that the determination of the single-channel amplitude was distorted by the rapid kinetics. The elementary characteristics of the other splice variant, TREK-2a (hTREK-2a; Lesage *et al.* 2000*b*) and of the rat orthologue of TREK-2a (rTREK-2a; Bang *et al.* 2000), have only been studied in inside-out patches. Interestingly, the conductance of these channels at positive potentials (allowing outward currents) was found to be much smaller (100 pS for hTREK-2a; 68 pS for rTREK-2a) than the values reported here. The reasons for this discrepancy are not clear. In the absence of external divalent cations, the conductance of TREK-2b and TREK-2c at negative potentials increased to 250–300 pS. The molecular mechanisms underlying the marked dependence of inward currents on the presence of divalent external cations (Fig. 6), which is also found in TASK-3 (Rajan *et al.* 2000), are not yet known.

The K_{2P} channels are generally characterized by short openings interrupted by short closures, which results in the typical 'flickery' appearance of single-channel recordings. The mean open time of TREK-2b and TREK-2c at −84 mV could be described by a single time constant of about 130 μs. The closed time distribution at the same potential showed at least two components, of which the shorter one was about 110 μs. The whole-cell current voltage relation of TREK-2b and TREK-2c in normal physiological salt solution (containing 5 mM K^+) was outwardly rectifying (Fig. 7), similar to TREK-2a (Lesage *et al.* 2000*b*). This outward rectification is most likely the result of (i) the asymmetrical K^+ concentrations and (ii) the voltage dependence of open probability (Lesage *et al.* 2000*b*; Bang *et al.* 2000).

Regulation of TREK-2 channels

The amplitude of the whole-cell current carried by TREK-2 channels could be increased by volatile anaesthetics (isoflurane, halothane and chloroform) and by externally applied lipids (linoleic acid and arachidonic acid). In this respect there was no difference between the two novel splice forms TREK-2b and TREK-2c and the data published previously for TREK-2a (Lesage *et al.* 2000*b*). This was to be expected since the three splice variants differ only in their N-terminus. At position 7 of TREK-2b there is a putative PKC phosphorylation site that is not present in TREK-2a and TREK-2c. However, both TREK-2b and TREK-2c could be inhibited by PMA, a non-specific activator of PKC. Furthermore, removal of the putative phosphorylation site by mutagenesis (construct TREK-2b T7A) did not cause a significant change in the effects of PMA. Thus, the putative phosphorylation site at position 7 is either not functional or the phosphorylation at this position has no effect on current amplitude.

In contrast, we found that activation of PKA by forskolin produced a significant decrease in whole-cell current. When the putative phosphorylation site was removed (construct S364A) the inhibitory effect of forskolin disappeared. These findings suggest that phosphorylation by PKA at position 364 of TREK-2b and TREK-2c (which corresponds to S359 in hTREK-2a) can inhibit the outward current of TREK-2 channels.

Possible alternative splicing in other K_{2P} channels

In the GenBank database several entries from TREK-1 and TRAAK channels from different species can be found which differ substantially in their N-terminal regions. This may indicate alternative splicing in other members of the TREK/TRAAK subfamily as well. For human TREK-1, two putative splice forms can be found in the GenBank database: AF129399 and AF171068 encode a shorter variant that was characterized in several studies (Fink *et al.* 1996; Meadows *et al.* 2000), AF004711 encodes another longer splice form (named TPKC1) isolated from human brain that also harbours 15 extra amino acids at the N-terminal part (Bockenhauer *et al.* 2001). Interestingly, the TREK-1 isoform that we isolated from rat brain has a similar N-terminal extension (accession number AF385401). Unfortunately, a genomic sequence for the first human TREK-1/*KCNK2* exons on chromosome 1 is still not available. For TRAAK there are database entries for mouse, rat and human. A yet unpublished human TRAAK isoform (AF247042) is significantly longer (26 amino acids) than the mouse and rat cDNAs (AF056492 and AF302842); the published human sequence (Lesage *et al.* 2000*a*) may therefore represent a different splice form.

Conclusions

The diversity of potassium currents in different cell types is determined not only by the number of different channel genes, but also by alternative splicing and heteromer formation of different subunits (Luneau *et al.* 1991; Butler *et al.* 1993; Attali *et al.* 1993; Shuck *et al.* 1994; Derst *et al.* 2001; Pan *et al.* 2001). Diversity of the K_{2P} channel family is partly determined by the relatively large number or different genes: about 50 K_{2P} channel genes were found in *Caenorhabditis elegans* (Wei *et al.* 1996), twelve K_{2P} channel genes were found in *Drosophila melanogaster* (Littleton & Ganetzki, 2000) and the number of K_{2P} channels in the human genome is at least 14. The results reported here show that alternative splicing of TREK-2, and possibly other K_{2P} channels, can further increase channel diversity. The cell-specific expression of different splice forms may play an important role in determining the functional properties of various neuronal and non-neuronal cell types.

REFERENCES

Attali, B., Lesage, F., Ziliani, P., Guillemare, E., Honore, E., Waldmann, R., Hugnot, J. P., Mattei, M. G., Lazdunski, M. & Barhanin, J. (1993). Multiple mRNA isoforms encoding the mouse cardiac Kv1.5 delayed rectifier K^+ channel. *Journal of Biological Chemistry* **268**, 24283–24289.

Bang, H., Kim, Y. & Kim, D. (2000). TREK-2, a new member of the mechanosensitive tandem-pore K^+ channel family. *Journal of Biological Chemistry* **275**, 17412–17419.

Bockenhauer, D., Zilberberg, N. & Goldstein, S. A. N. (2001). KCNK2: reversible conversion of a hippocampal potassium leak into a voltage-dependent channel. *Nature Neuroscience* **4**, 486–491.

Butler, A., Tsunoda, S., McCobb, D. P., Wei, A. & Salkoff, L. (1993). mSlo, a complex mouse gene encoding "maxi" calcium-activated potassium channels. *Science* **261**, 221–224.

Chavez, R. A., Gray, A. T., Zhao, B. B., Kindler, C. H., Mazurek, M. J., Mehta, Y., Forsayeth, J. R. & Yost, C. S. (1999). TWIK-2, a new weak inward rectifying member of the tandem pore domain potassium channel family. *Journal of Biological Chemistry* **274**, 7887–7892.

Decher, N., Maier, M., Dittrich, W., Gassenhuber, J., Brüggemann, A., Busch, A. E. & Steinmeyer, K. (2001). Characterization of TASK-4, a novel member of the pH-sensitive, two-pore domain potassium channel family. *FEBS Letters* **492**, 84–89.

Derst, C., Karschin, C., Wischmeyer, E., Hirsch, J. R., Preisig-Muller, R., Rajan, S., Engel, H., Grzeschik, K. H., Daut, J. & Karschin, A. (2001). Genetic and functional linkage of Kir5.1 and Kir2.1 channel subunits. *FEBS Letters* **491**, 305–311.

Duprat, F., Lesage, F., Fink, M., Reyes, R., Heurteaux, C. & Lazdunski, M. (1997). TASK, a human background K^+ channel to sense external pH variations near physiological pH. *EMBO Journal* **16**, 5464–5471.

Fink, M., Duprat, F., Lesage, F., Reyes, R., Romey, G., Heurteaux, C. & Lazdunski, M. (1996). Cloning, functional expression and brain localization of a novel unconventional outward rectifier K^+ channel. *EMBO Journal* **15**, 6854–6862.

Fink, M., Lesage, F., Duprat, F., Heurteaux, C., Reyes, R., Fosset, M. & Lazdunski, M. (1998). A neuronal two P domain K^+ channel stimulated by arachidonic acid and polyunsaturated fatty acids. *EMBO Journal* **17**, 3297–3308.

Girard, C., Duprat, F., Terrenoire, C., Tinel, N., Fosset, M., Romey, G., Lazdunski, M. & Lesage, F. (2001). Genomic and functional characteristics of novel human pancreatic 2P domain K^+ channels. *Biochemical and Biophysical Research Communications* **282**, 249–256.

Goldstein, S. A., Bockenhauer, D., O'Kelly, I. & Zilberberg, N. (2001). Potassium leak channels and the KCNK family of two-P-domain subunits. *Nature Reviews Neuroscience* **2**, 175–184.

Gray, A. T., Zhao, B. B., Kindler, C. H., Winegar, B. D., Mazurek, M. J., Xu, J., Chavez, R. A., Forsayeth, J. R. & Yost, C. S. (2000). Volatile anesthetics activate the human tandem pore domain baseline K^+ channel KCNK5. *Anesthesiology* **92**, 1722–1730.

Karschin, C., Wischmeyer, E., Preisig-Müller, R., Rajan, S., Derst, C., Grzeschik, K.-H., Daut, J. & Karschin, A. (2001). Expression pattern in brain of TASK-1, TASK-3, and a tandem pore domain K^+ channel subunit, TASK-5, associated with the central auditory nervous system. *Molecular and Cellular Neuroscience* **18**, 632–648.

Kim, Y., Bang, H. & Kim, D. (2000). TASK-3, a new member of the tandem pore K^+ channel family. *Journal of Biological Chemistry* **275**, 9340–9347.

Kim, D., Fujita, A., Horio, Y. & Kurachi, Y. (1998). Cloning and functional expression of a novel cardiac two-pore background K^+ channel (cTBAK-1). *Circulation Research* **82**, 513–518.

Kim, D. & Gnatenco, C. (2001). TASK-5, a new member of the tandem-pore K^+ channel family. *Biochemical and Biophysical Research Communications* **284**, 923–930.

Lesage, F., Guillemare, E., Fink, M., Duprat, F., Lazdunski, M., Romey, G. & Barhanin, J. (1996*a*). TWIK-1, a ubiquitous human weakly inward rectifying K^+ channel with a novel structure. *EMBO Journal* **15**, 1004–1011.

Lesage, F. & Lazdunski, M. (2000). Molecular and functional properties of two-pore-domain potassium channels. *American Journal of Physiology* **279**, F793–801.

Lesage, F., Maingret, F. & Lazdunski, M. (2000*a*). Cloning and expression of human TRAAK, a polyunsaturated fatty acids-activated and mechano-sensitive K^+ channel. *FEBS Letters* **471**, 137–140.

Lesage, F., Reyes, R., Fink, M., Duprat, F., Guillemare, E. & Lazdunski, M. (1996*b*). Dimerization of TWIK-1 K^+ channel subunits via a disulfide bridge. *EMBO Journal* **15**, 6400–6407.

Lesage, F., Terrenoire, C., Romey, G. & Lazdunski, M., (2000*b*). Human TREK2, a 2P domain mechano-sensitive K^+ channel with multiple regulations by polyunsaturated fatty acids, lysophospholipids and Gs, Gi, and Gq protein-coupled receptors. *Journal of Biological Chemistry* **275**, 28398–28405.

Littleton, J. T. & Ganetzky, B. (2000). Ion channels and synaptic organization: analysis of the Drosophila genome. *Neuron* **26**, 35–43.

Luneau, C. J., Williams, J. B., Marshall, J., Levitan, E. S., Oliva, C., Smith, J. S., Antanavage, J., Folander, K., Stein, R. B., Swanson, R., Kaczmarek, L. K. & Buhrow, S. A. (1991). Alternative splicing contributes to K^+ channel diversity in the mammalian central nervous system. *Proceedings of the National Academy of Sciences of the USA* **88**, 3932–3936.

Maingret, F., Fosset, M., Lesage, F., Lazdunski, M. & Honoré, E. (1999*a*). TRAAK is a mammalian neuronal mechano-gated K^+ channel. *Journal of Biological Chemistry* **274**, 1381–1387.

Maingret, F., Patel, A. J., Lesage, F., Lazdunski, M., Honoré, E. (1999*b*). Mechano- or acid stimulation, two interactive modes of activation of the TREK-1 potassium channel. *Journal of Biological Chemistry* **274**, 26691–26696.

Maingret, F., Patel, A. J., Lesage, F., Lazdunski, M. & Honoré, E. (2000). Lysophospholipids open the two-pore domain mechano-gated K^+ channels TREK-1 and TRAAK. *Journal of Biological Chemistry* **275**, 10128–10133.

Meadows, H. J., Benham, C. D., Cairns, W., Gloger, I., Jennings, C., Medhurst, A. D., Murdock, P. & Chapman, C. G. (2000). Cloning, localisation and functional expression of the human orthologue of the TREK-1 potassium channel. *Pflügers Archiv* **439**, 714–722.

Millar, J. A., Barratt, L., Southan, A. P., Page, K. M., Fyffe, R. E. W., Robertson, B. & Mathie, A. (2000). A functional role for the two-pore domain potassium channel TASK-1 in cerebellar granule neurons. *Proceedings of the National Academy of Sciences of the USA* **97**, 3614–3618.

Neher, E. (1992). Correction for liquid junction potentials in patch clamp experiments. In *Methods in Enzymology*, vol. 207, *Ion Channels*, ed. Rudy, B. & Iverson, L.E., pp. 123–131. Academic Press, San Diego.

Pan, Z., Selyanko, A. A., Hadley, J. K., Brown, D. A., Dixon, J. E. & McKinnon, D. (2001). Alternative splicing of KCNQ2 potassium channel transcripts contributes to the diversity of M-currents. *Journal of Physiology* **531**, 347–358.

Patel, A. J., Honoré, E., Maingret, F., Lesage, F., Fink, M., Duprat, F. & Lazdunski, M. (1998). A mammalian two pore domain mechano-gated S-like K^+ channel. *EMBO Journal* **17**, 4283–4290.

Patel, A. J., Honoré, E., Lesage, F., Fink, M., Romey, G. & Lazdunski, M. (1999*a*). Inhalational anesthetics activate two-pore-domain background K^+ channels. *Nature Neuroscience* **2**, 422–426.

Patel, A. J. & Honoré, E. (2001). Properties and modulation of mammalian 2P domain K^+ channels. *Trends in Neurosciences* **24**, 339–346.

Patel, A. J., Maingret, F., Magnone, V., Fosset, M., Lazdunski, M. & Honoré, E. (1999*b*). TWIK-2, an inactivating 2P domain K^+ channel. *Journal of Biological Chemistry* **275**, 28722–28730.

Rajan, S., Wischmeyer, E., Karschin, C., Preisig-Müller, R., Grzeschik, K.-H., Daut, J., Karschin, A. & Derst, C. (2001). THIK-1 and THIK-2, a novel subfamily of tandem pore domain K^+ channels. *Journal of Biological Chemistry* **276**, 7302–7311.

Rajan, S., Wischmeyer, E., Liu, G. X., Preisig-Müller, R., Daut, J., Karschin, A. & Derst, C. (2000). TASK-3, a novel tandem pore domain acid-sensitive K^+ channel. An etracellular histidine as pH sensor. *Journal of Biological Chemistry* **275**, 16650–16657.

Reyes, R., Duprat, F., Lesage, F., Fink, M., Salinas, M., Farman, N. & Lazdunski, M. (1998). Cloning and expression of a novel pH-sensitive two pore domain K^+ channel from human kidney. *Journal of Biological Chemistry* **273**, 30863–30869.

Salinas, M., Reyes, R., Lesage, F., Fosset, M., Heurteaux, C., Romey, G. & Lazdunski, M. (1999). Cloning of a new mouse two-P domain channel subunit and a human homologue with a unique pore structure. *Journal of Biological Chemistry* **274**, 11751–11760.

Schafer, J. A., Watkins, M. L., Li, L., Herter, P., Haxelmans, S. & Schlatter, E. (1997). A simplified method for isolation of large numbers of defined nephron segments. *American Journal of Physiology* **273**, F650–657.

Shuck, M. E., Bock, J. H., Benjamin, C. W., Tsai, T. D., Lee, K. S., Slightom, J. L. & Bienkowski, M. J. (1994). Cloning and characterization of multiple forms of the human kidney ROMK potassium channel. *Journal of Biological Chemistry* **269**, 24261–24270.

Sirois, J. E., Lei, Q., Talley, E. M., Lynch, C. III & Bayliss, D. A. (2000). The TASK-1 two-pore domain K^+ channel is a molecular substrate for neuronal effects of inhalation anesthetics. *Journal of Neuroscience* **20**, 6347–6354.

Talley, E. M., Lei, Q., Sirois, J. E. & Bayliss, D. A. (2000). TASK-1, a two-pore domain K^+ channel, is modulated by multiple neurotransmitters in motoneurons. *Neuron* **25**, 399–410.

Talley, E. M., Solorzano, G., Lei, Q., Kim, D. & Bayliss, D. A. (2001). CNS distribution of members of the two-pore-domain (KCNK) potassium channel family. *Journal of Neuroscience* **21**, 7491–7505.

Wei, A., Jegla, T. & Salkoff, L. (1996). Eight potassium channel families revealed by the *C. elegans* genome project. *Neuropharmacology* **35**, 805–829.

Acknowledgements

This work was supported by the Deutsche Forschungsgemeinschaft (grants Da177/7-3 and Ka1175/1-3), by the Ernst-und-Berta-Grimmke Stiftung and by the P. E. Kempkes-Stiftung. We thank Regina Preisig-Müller and Sindhu Rajan for useful discussions. The excellent technical help of Tanja Haase, H. Wegener and Anette Hennighausen is gratefully acknowledged.